

# APPLICATION OF COMPUTER IDENTIFICATION AND LOCATION ALGORITHM IN SMALL FAR INFRARED TARGET RECOGNITION OF SHIP UNDER SURGE INTERFERENCE

Renping Zhu

Department of Admission and Employment Office, Nanchang University, Nanchang 330031, China

## ABSTRACT

*The small far infrared target of ship in surge interference is easy to have visual deviation causing the low accuracy of target positioning and the bad target identification performance. In order to improve the accuracy of far small infrared targets recognition of ship under surge interference, this paper proposed far small infrared target recognition algorithm of ship based on distributed target position estimation and DOA location in computer vision model for constructing coherent distributed source array model of far small infrared target distribution of ship. This algorithm used MUSIC algorithm for the beamforming processing of far small infrared target echo model of ship. Combined with the adaptive filtering algorithm we carried out the surge interference suppression and the estimation of central direction of arrival and angle spread of far small infrared target of ship through multidimensional spectrum peak searching algorithm, realizing the joint estimation of distance of ship target, DOA and frequency parameters, so as to realize the accurate positioning and recognition of targets. Simulation results show that using this method for the far small infrared target recognition of ship under surge interference, the spectral peak sharpness of spectral peak search of target position is high, side-lobe suppression performance is good, which shows the high accuracy of target position estimation and location, the accuracy and anti-interference performance of far small infrared target recognition of ship is good, and has superior performance.*

**Keywords:** Computer identification; Target position estimation; Location; Ship; Infrared target; Surge interference

## INTRODUCTION

Modern war is a high-tech war. The development of ship target recognition technology is relatively slow. Besides the high degree of military secrecy, the background of the underwater environment is extremely complex. The impact of environmental interference on the working performance of underwater weapon systems and ship target recognition can not be ignored [1].

Ship target recognition is divided into active recognition and passive recognition according to the guidance performance of assault weapon. the ship far small infrared target recognition uses a variety of parameters of target information as feature vectors [2-4], such as in ship small far infrared target recognition, reflection echo of ship target

is the function of the target type, distance and direction, which includes the characteristics information such as echo broadening, amplitude, phase, reflection coefficient, target scale, energy spectrum [5]. Common signal features are: AR model parameters, Fourier power spectrum, wavelet transform parameters. Combined with DOA target location analysis and beamforming method [6-10], we achieve accurate positioning detection and identification of ship targets. For passive target recognition of ship radiated noise, the method includes LOFAR spectrum and the high order spectrum [11]. The feature extraction of nonlinear feature of ship radiated noise mainly uses the fractal, limit cycles, chaos and other new mathematical methods. For above methods under surge

interference, the identification accuracy is not high, the stability is not good [12].

Aiming at the above problems, this paper proposed far small infrared target recognition algorithm of ship based on distributed target position estimation and DOA location in computer vision model for constructing coherent distributed source array model of far small infrared target distribution of ship. This algorithm used MUSIC algorithm for the beamforming processing of far small infrared target echo model of ship. Then, combined with the adaptive filtering algorithm we carried out the surge interference suppression and the estimation of central direction of arrival and angle spread of far small infrared target of ship through multidimensional spectrum peak searching algorithm, realizing the joint estimation of distance of ship target, DOA and frequency parameters, so as to realize the accurate positioning and recognition of targets. Finally, we took the actual ship target information collected data as the test sample for identification performance test, which shows the superior performance of the proposed method in improving the accuracy of ship target recognition, and got the effectiveness conclusion.

## ARRAY MODEL OF SHIP FAR SMALL INFRARED TARGET DISTRIBUTION

### SHIP FAR SMALL INFRARED TARGET DISTRIBUTED MODELING

In the actual environment, the target will occupy a certain volume, so this does not idealize itself into a single point in the space. For such target, the received signal is no longer the echo of a single point source, but rather the superposition of multiple spatially similar point source echoes. Such target is called a distributed target [13-15]. We construct near field source model of ship target echo, assuming that equidistant line array which is composed of  $N = 2P$  array elements receives  $I$  near field sources, as shown in Fig. 1.

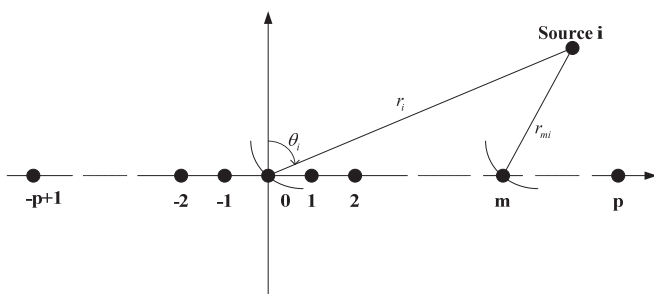


Fig. 1. Uniform linear array target distribution model of near infrared source of ship far small infrared target.

Let the array element coordinates of the ship far small infrared target at the center of the array be 0, taking it as the

phase reference point, then the echo signal of the receiving ship target of the  $m$ -th array element can be expressed as:

$$x_m(t) = \sum_{i=1}^I s_i(t) e^{j\varphi_{mi}} + n_m(t), -p+1 \leq m \leq p \quad (1)$$

Among them,  $s_i(t)$  is the complex envelope of the  $i$ th far small infrared target source of ship.  $x_m(t)$  is the observation signal received by the array element  $m$ .  $n_m(t)$  is the additive noise on the element  $m$ .  $\varphi_{mi}$  is the phase difference of the source  $i$  signal received by the element  $m$  relative to the reference element. The analytic expression of  $\varphi_{mi}$  is not difficult to get:

$$\varphi_{mi} = \frac{2\pi r_i}{\lambda} \left( \sqrt{1 + \frac{m^2 d^2}{r_i^2}} - \frac{2md \sin \theta_i}{r_i} - 1 \right) \quad (2)$$

Among them,  $r_i$ ,  $\theta_i$  is the distances of the  $i$ th near field source (relative to the reference element) and the DOA of the ship far small infrared target to be estimated, and  $\lambda$  is the wavelength of the source  $d$  is the array element interval.

$$\varphi_{mi} \approx \gamma_i m + \phi_i m^2 \quad (3)$$

$$\gamma_i = -2\pi \frac{d}{\lambda} \sin \theta_i, \quad \phi_i = \pi \frac{d^2}{\lambda r_i} \cos^2 \theta_i \quad (4)$$

Thus, the time delay phase difference is composed of two parts: the first is the linear term of array elements location, which is same as general far-field signal model; the second is the quadratic nonlinear term of array elements location, which is determined by DOA and distance parameters, this term increases with the decrease of near field sources [16], otherwise, when the distance tends to infinity, the nonlinear term is zero, the formula (3) degenerates into to far-field signal time delay difference model.

The  $N$ -dimension vector  $x(t)$  is used to represent the ship far small infrared target array output data vector, thus:

$$x(t) = As(t) + n(t) \quad (5)$$

Among them,

$$x(t) = [x_{-p+1}(t), x_{-p+2}(t), \dots, x_p(t)]_{N \times 1}^T \quad (6)$$

$$s(t) = [s_1(t), s_2(t), \dots, s_I(t)]_{I \times 1}^T \quad (7)$$

$$n(t) = [n_{-p+1}(t), n_{-p+2}(t), \dots, n_p(t)]_{N \times 1}^T \quad (8)$$

$$A = [a(\theta_1, r_1), a(\theta_2, r_2), \dots, a(\theta_I, r_I)]_{N \times I} \quad (9)$$

$$a(\theta_i, r_i) = [\exp(j[(-P+1)\gamma_i + (-P+1)^2\phi_i]), \exp(j[(-P+2)\gamma_i + (-P+2)^2\phi_i]), \dots, \exp(j[P\gamma_i + P^2\phi_i])]_{N \times 1}^T \quad (10)$$

Among them,  $1 \leq i \leq I$ , the  $i$ -th column vector  $a(\theta_i, r_i)$  of the matrix  $A$  is called the direction vector of the source  $i$  signal of the ship far small infrared target (also called rudder vector). The matrix  $A$  is called the direction matrix of the array (or response matrix). It can also be called the array manifold. The information of the ship far small infrared target can be used to determine the direction vector.

The distance  $r$  of the near field source of ship far small infrared target distribution relative to array center can be approximated:

$$r \leq 2D^2 / \lambda \quad (11)$$

Among them,  $D$  is the maximum aperture of the receiving array.  $\lambda = c / f$  indicates the operating wavelength corresponding to the central frequency  $f$  of the source.

## A COHERENT SOURCE OF TARGET LOCATION RECOGNITION

Its covariance matrix is:

$$R_z = E[z(t)z(t)^H] = R_s(\psi) + R_n \quad (12)$$

Among them,

$$R_s(\psi) = \sum_{i=1}^p \sum_{j=1}^p \int_{-\pi/2}^{\pi/2} \int_{-\pi/2}^{\pi/2} a(\theta) p_{ij}(\theta, \theta'; \psi_i, \psi_j) a^H(\theta') d\theta d\theta' \quad (13)$$

$$p_{ij}(\theta, \theta'; \psi_i, \psi_j) = E[s_i(\theta, \psi_i) s_j(\theta', \psi_j)] \quad (14)$$

is called the angle cross-correlation kernel, it reflects the degree of correlation between the echo signal in different angles. If the components of direction of arrival between different distribution source is irrelevant [19], the angle cross-correlation kernel can be simplified to  $p_{ij}(\theta, \theta'; \psi_i, \psi_j) = p_i(\theta, \theta'; \psi_i) \delta_{ij}$ , this shows that angle cross-correlation kernel is zero at  $i \neq j$ ,  $p_i(\theta, \theta'; \psi_i) \delta_{ij} = E[s_i(\theta, \psi_i) s_i^*(\theta', \psi_i)]$  is called angle cross-correlation kernel of the  $i$ th distribution source. At this time,

$$R_s(\psi) = \sum_{i=1}^p \int_{-\pi/2}^{\pi/2} \int_{-\pi/2}^{\pi/2} a(\theta) p_i(\theta, \theta'; \psi_i) a^H(\theta') d\theta d\theta'$$

In surge interference, for the coherent source in source,  $s(\theta; \psi_i) = \gamma_i g(\theta; \psi_i)$ ,  $\gamma_i$  is the random variable.  $g(\theta; \psi_i)$  is deterministic complex valued function. For coherent sources, the autocorrelation kernel of the angle is  $p(\theta, \theta'; \psi) = \eta g(\theta, \psi) g^*(\theta', \psi)$ , among them  $\eta = E[\gamma\gamma^*]$ . For the distribution source of signals incoherent from different angles in the same target, the autocorrelation kernel of the angle is  $p(\theta, \theta'; \psi) = p(\theta; \psi) \delta(\theta - \theta')$ ,  $p(\theta; \psi)$  is called the

angle power density of the distribution source. At this time, the covariance matrix of ship far small infrared target echo signal:  $R_s(\psi) = \sum_{i=1}^p \int_{-\pi/2}^{\pi/2} a(\theta) p(\theta; \psi_i) a^H(\theta) d\theta$ .

For modeling, the target model of related source is divided into coherent source model and partial correlation source model [20].

The so-called coherent source is that there is a strong correlation between the signals from different directions in the same target body. The angular density function  $s_i(\theta - \theta_i, t)$  can be expressed as:

$$s_i(\theta - \theta_i, t) = s_i(t) g_i(\theta - \theta_i) \quad (15)$$

$s_i(t)$  is the random signal, usually, the distribution of distributed targets is symmetrical. Then supposing that  $g_i(\theta - \theta_i)$  is the deterministic function taking  $\theta_i$  as the symmetry center with a single peak.  $g_i(\theta - \theta_i)$  which satisfies  $\int_{-\pi}^{\pi} g_i(\theta - \theta_i) d\theta = 1$  is called distribution function of the angular signal of the  $i$ -th distributed target signal source,  $\theta_i$  is the central direction of arrival of the distributed target, which is the parameter to be estimated. When the mathematical form of the angular signal distribution function  $g_i(\theta - \theta_i)$  (e.g., Gaussian distribution) is known, its shape is determined by unknown distributed parameters, and the observation data  $Z(t)$  of array at  $t$  time can be represented as:

$$z(t) = \sum_{i=1}^p s_i(t) b_i(\theta_i) + n(t) \quad (16)$$

Among them,  $b_i(\theta_i)$  is the direction vector of  $i$ th distributed target, which can be expressed as:

$$b_i(\theta_i) = \int_{-\pi}^{\pi} a(\theta) g_i(\theta - \theta_i) d\theta \quad (17)$$

Among them  $i = 1, 2, \dots, p$ ,  $p$  is the distributed target number.  $b_i(\theta_i)$  is determined by the mathematical form of angular signal distribution function of ship far small infrared target signal source and unknown distributed parameter, which is  $M$ -order direction vector.  $M$  is array element number of ship far small infrared targets in the array manifold vector. From  $\int_{-\pi}^{\pi} g_i(\theta - \theta_i) d\theta = 1$ , we can see the first element of the direction vector  $b_i(\theta_i)$  is 1. When  $g_i(\theta - \theta_i)$  is the  $\delta(\theta - \theta_i)$  function,  $b_i(\theta_i) = a(\theta)$ , the distributed ship far small infrared target is degraded into point target [21].

The direction vector of the distributed target is obtained, and  $b_i(\theta_i)$  can also be understood as a generalized array flow pattern.  $b_i(\theta_i)$  is known, we can construct the model of the array receiving data by following formulas:

$$a(\theta) = \left[ 1, e^{-j2\pi fd \sin(\theta)/c}, e^{-j2\pi fd \sin(\theta)/c}, \dots, \exp^{-j(M-1) \cdot 2\pi fd \sin(\theta)/c} \right] \quad (18)$$

$f$  is the center frequency of signal.  $c$  is the acoustic velocity.  $d$  is the array element spacing.

At this time, the generalized flow pattern vector of the distributed source model that the the angular signal distribution function is Gaussian distribution can be obtained by formula (17):

$$b_i(\theta_i) = \left[ 1, e^{-\frac{\sigma_{\theta_i}^2}{2}} e^{-j2\pi f d \sin(\theta)/c}, \dots, e^{-(M-1)\frac{\sigma_{\theta_i}^2}{2}} e^{-j(M-1)2\pi f d \sin(\theta)/c} \right] \quad (19)$$

Then the mathematical model of array reception can be obtained according to (16).

## BEAMFORMING OF MUSIC ALGORITHM AND TARGET ECHO

### IMPROVEMENT OF MUSIC ALGORITHM

Raich R proposed MUSIC (Multiple Signal Classification) algorithm, this algorithm is basic algorithm for target beamforming and orientation positioning recognition[22]. In this paper, the traditional one-dimensional MUSIC method is extended to two-dimensional MUSIC method, realizing the joint estimation of the near field source distance and azimuth angle two-dimensional parameters of the ship far small infrared targets [23]. According to above geometry model of coherent distribution of ship target and the basic assumption of parameter estimation, the covariance matrix  $R_x$  of observation signal is defined as:

$$R_x = E\{x(t)x^H(t)\} = AE\{s(t)s^H(t)\}A^H + E\{n(t)n^H(t)\} = AR_sA^H + R_n \quad (20)$$

Among them,  $R_x$  is the H matrix. The rank is  $N$ .  $R_s$  is the covariance matrix of signal. The rank is  $I$ .  $R_n = \sigma^2 I_N$  is the noise covariance matrix.  $I_N$  is the  $N \times N$  unit matrix. For finite length sample,  $t = 1, 2, \dots, K$ ,  $K$  is the number of snapshots (snapshots, i.e. a sampling point),  $R_x$  can be estimated following formula:

$$\hat{R}_x = \frac{1}{K} \sum_{t=1}^K x(t)x^H(t) \quad (21)$$

We carry out the eigendecomposition on the covariance matrix  $R_x$  of the observation signal:

$$R_x V = \Lambda V \quad (22)$$

Among them,  $\Lambda = \text{diag}[\rho_1, \rho_2, \dots, \rho_N]$  is the diagonal matrix consisting of the eigenvalues in descending order, that is:

$$\rho_1 \geq \rho_2 \geq \dots \geq \rho_I > \rho_{I+1} = \rho_{I+2} = \dots = \rho_M = \sigma^2 \quad (23)$$

$V = [v_1, v_2, \dots, v_I, v_{I+1}, v_{I+2}, \dots, v_N]$  is the eigenvector matrix corresponding to the eigenvalue  $\{\rho_i\}_{1 \leq i \leq N}$ , the signal subspace

and the noise subspace which are composed of eigenvectors are respectively defined as:

$$V_s = [v_1, v_2, \dots, v_I]_{N \times I}, \quad V_n = [v_{I+1}, v_{I+2}, \dots, v_N]_{N \times (N-I)} \quad (24)$$

Using the orthogonality of the signal subspace  $V_s$  and the noise subspace  $V_n$ , the formula (22) can be derived:

$$R_x V_n = \sigma^2 V_n \quad (25)$$

Formula (18) postmultiplies  $V_n$ , we get:

$$R_x V_n = (AR_sA^H + \sigma^2 I_N) V_n \quad (26)$$

Combining expressions (21) and formula (22), we can get:

$$A^H V_n V_n^H A = 0 \quad (27)$$

Therefore, the spectral function of the MUSIC method is:

$$P(\theta, r) = \left| a^H(\theta, r) V_n V_n^H a(\theta, r) \right|^{-1} \quad (28)$$

Among them,  $a(\theta, r)$  is all possible direction vector. Through two-dimensional spectral peak search of azimuth and distance for the spectral function  $P(\theta, r)$ , the peak value is the position information  $\{\theta_i, r_i\}_{1 \leq i \leq I}$  of the near field source.

Using the improved MUSIC algorithm for the beamforming processing of ship far small infrared target echo model [24], we get the echo vector  $b(k)$  of ship far small infrared target in surge interference, which can be expressed as the weighted combination of each point source on the continuous direction, that is:

$$b(k) = \int_{-\pi}^{\pi} f(\theta, k) a(\theta) d\theta \quad (29)$$

Among them,  $a(\theta) = [1, e^{-j\pi \sin \theta}, e^{-j2\pi \sin \theta}, \dots, e^{-j(M-1)\pi \sin \theta}]^T$  is the conventional  $M \times 1$ -order point source array flow pattern vector.  $f(\theta, k)$  is a random angle-time weighting function.

### BEAM FORMING ALGORITHM

Now, some parts of the relevant distribution source (PCD) can be defined as the point target in a relatively short period of observation interval, we use a weighted correlation function for the formation of the autocorrelation function, which only depends on the discrete time interval of  $l$ , and for the different angle, they all are zero.

$$E[f(\theta, k) f^*(\theta', k+l)] = \gamma_f(\theta, l) \delta(\theta - \theta'), \forall l \in Z \quad (30)$$

$\gamma_f(\theta, l)$  is the correlation function of  $f(\theta, k)$ , which is often called as the correlation kernel of the angle-time(ATCK). In the beamforming, zero-time related ICD type and full time related FCD type model can be regarded as the point target of PCD type of additional conditions [25-27]. The decision statistic of beam forming is obtained:

$$\begin{aligned}
ICD: \gamma_f(\theta, l) &= \gamma_f(\theta) \delta(l), \gamma_f(\theta) = \gamma_f(\theta, 0) \\
FCD: \gamma_f(\theta, l) &= \gamma_f(\theta), \forall l \in Z
\end{aligned}
\tag{31}$$

From above formulas, we can see that the statistical properties of the angular time weighting function  $f(\theta, k)$  can influence the statistical properties of the channel vectors of the PCD source. For  $b(k)$ , there is:

$$\begin{aligned}
b(k) &\in N(0_{M \times 1}, R_b), R_b = R_b(0) \\
R_b(l) &= E[b(k)b^H(k+l)] = \int_{-\pi}^{\pi} \gamma_f(\theta, l) a(\theta) a^H(\theta) d\theta
\end{aligned}
\tag{32}$$

For the ICD and FCD sources, the channel vector can also be described as the closed Gauss random vector of zero mean complex values, corresponding to the ICD and FCD distribution sources, and the correlation matrix of  $b(k)$  has the following properties:

$$\begin{aligned}
ICD: R_b(l) &= R_b \delta_l; (R_b(l) = E[b(k)b^H(k+l)]) \\
FCD: R_b(l) &= R_b, \forall l \in Z
\end{aligned}
\tag{33}$$

From the above analysis, we can see that ATCK contains the angular and temporal characteristics of the PCD source. From the previous analysis about the ICD and FCD sources, the focus of the study will be focused on how to determine the ATCK model by a limited number of parameters. Specially, ATCK can be written as:

$$\gamma_f(\theta, l) \Rightarrow \gamma_f(\theta, l | \xi), \xi = [\phi^T, \tau^T]^T
\tag{34}$$

In order to easily understand the concept of PCD model, a simple first-order autoregressive AR model is firstly proposed for the channel vector of surge interference.

$$b(k) = \alpha b(k-1) + \sqrt{1-\alpha^2} w(k)
\tag{35}$$

$\alpha$  represents the time correlation of two adjacent surge interference channel vector sampling values, and driven vector  $w(k)$  includes zero mean, independent identically distributed complex valued Gaussian random vector, these vectors are characterized by angular power density function of Gaussian shape.

$$\begin{aligned}
w(k) &\in N(0_{M \times 1}, R_w), R_w = R_w(0) \\
R_w(l) &= E[w(k)w^H(k+l)] \\
&= \int_{-\pi}^{\pi} \left[ \delta_l \cdot \frac{1}{\Delta\sqrt{2\pi}} e^{-\frac{(\theta-\theta_0)^2}{2\Delta^2}} \right] a(\theta) a^H(\theta) d\theta
\end{aligned}
\tag{36}$$

In formulas, two parameters  $\theta_0$  and  $\Delta$  represent the mean of angle and the angle standard deviation respectively.

## SURGE INTERFERENCE SUPPRESSION FILTER PROCESSING

On the basis of beamforming processing, the adaptive filtering algorithm is used to suppress the surge interference, and the filtering structure model of surge interference suppression is constructed, as shown in Fig. 2.

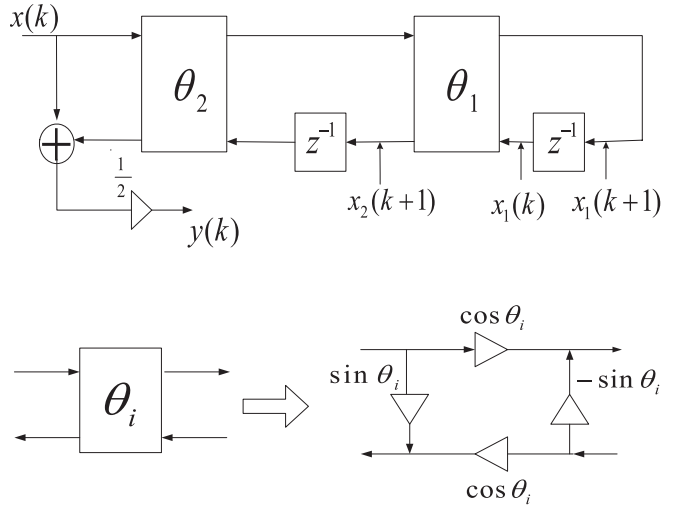


Fig. 2. Filtering structure of surge interference suppression.

The adaptive gradient algorithm is used for the adaptive iteration, and the selection of  $\theta_1(k)$  should minimize the energy of output signal of filter, so  $y(k)y^*(k)$  is the minimum. Here, “\*” represents complex conjugate. Thus, the iterative formula of the surge suppression filter of ship far small infrared target recognition is obtained:

$$\theta_1(k+1) = \theta_1(k) - \mu \text{Re}[y(k)\varphi^*(k)]
\tag{37}$$

Among them,  $\mu$  is the parameter of the controllable convergence rate and accuracy, which is called step length.  $\varphi(k)$  is the difference of  $y(k)$  output to parameter  $\theta_1(k)$ , which is called the gradient signal, and it is generated by the input signal  $u(k)$  passing through the following transfer function:

$$H_B(z) = \frac{(1 + \sin \theta_2) \cos \theta_1(k) \cos \theta_2 z^{-1}}{\cos \theta_2 (1 + \sin \theta_1(k)(1 + \sin \theta_2) z^{-1} + \sin \theta_2 z^{-2})} G(z)
\tag{38}$$

Among them,

$$G(z) = \frac{1 - \sin \theta_2}{2} \frac{1 - z^{-2}}{1 + \sin \theta_1(k)(1 + \sin \theta_2) z^{-1} + \sin \theta_2 z^{-2}}
\tag{39}$$

For the convergence speed of acceleration algorithms, the corresponding complex number algorithm is proposed on the basis of this algorithm. The iterative formula of its parameter  $\theta_1$  is

$$\theta_1(k+1) = \theta_1(k) - \mu \text{Re}[y(k)x_1^*(k)]
\tag{40}$$

Among them,  $x_i(k)$  is called a reduced gradient signal, which is generated after the input signal  $u(k)$  passes through the following transfer function:

$$H'_B(z) = \frac{\cos \theta_1(k) \cos \theta_2 z^{-1}}{1 + \sin \theta_1(k)(1 + \sin \theta_2)z^{-1} + \sin \theta_2 z^{-2}} \quad (41)$$

The filter output  $y(k)$  and the gradient signal  $\varphi(k)$  can be represented as

$$y(k) = s_1(k) + n_1(k), \quad \varphi(k) = s_2(k) + n_2(k) \quad (42)$$

$$s_1(k) = AA_{H_H} e^{j(\Omega k + \theta_H)}, \quad s_2(k) = AA_{H_B} e^{j(\Omega k + \theta_{H_B})} \quad (43)$$

For gradient algorithms,  $A_H$ ,  $A_{H_B}$  and  $\theta_H$ ,  $\theta_{H_B}$  are the amplitude response and phase response of the transmission function of filter  $H(z)$  and  $H_B(z)$ , respectively. Through adaptive filtering, the suppression of surge interference in ship far small infrared target recognition has been realized.

## REALIZATION OF TARGET LOCATION ALGORITHM AND COMPUTER INTELLIGENT RECOGNITION OF SHIP TARGET

### MULTIDIMENSIONAL SPECTRAL PEAK SEARCH OF SHIP FAR SMALL INFRARED TARGET INFRARED TARGET

This paper proposed the ship far small infrared target recognition algorithm based on distributed target position estimation and DOA location [28,29]. Using the multidimensional spectrum peak search algorithm for central direction of arrival and extension angle estimation of far small infrared target of ship, we build the distributed target signal source model through a certain number of point target signal source, and construct the VEC-MUSIC multidimensional spectrum peak search algorithm. Supposing that there is a narrowband distributed source. It consists of a large number of scattering points around the source, the signal of receiving end can be expressed as the vector form:

$$x(t) = s(t) \sum_{n=1}^L \gamma_n(t) a(\theta + \tilde{\theta}_n(t)) + n(t) = s(t) v(t, \theta, \sigma_\theta) + n(t) \quad (44)$$

Among them,  $s(t)$  is the signal reflected from the ship far small infrared target distributed source.  $\gamma_n$  is the random gain of each signal, and  $\tilde{\theta}_n$  is the random angle offset relative to DOA. The probability density function of  $\tilde{\theta}_n$  is  $p(\tilde{\theta}; \sigma_\theta)$ , and  $\sigma_\theta$  is the standard deviation of the random angular offset  $\tilde{\theta}_n$ . Assuming that the gain factor  $\gamma_n$  is independent and zero mean, and  $E[|\gamma_n|^2] = 1/L$ . assuming

that the receiving array is the uniform linear array, then  $a(\theta) = [1, e^{-j2\pi\Delta \sin \theta}, \dots, e^{-j(M-1)2\pi\Delta \sin \theta}]^T$ .

In addition, the above model can be described as an integral form, and the array reception signal of the ship far small infrared target positioning recognition can be expressed as:

$$x(t) = s(t) \int_0^{2\pi} \gamma(\tilde{\theta}; t) a(\theta + \tilde{\theta}) d\tilde{\theta} + n(t) = s(t) v(t, \theta, \sigma_\theta) + n(t) \quad (45)$$

$\gamma(\tilde{\theta})$  is stochastic, and  $E[\gamma(\tilde{\theta}_1)\gamma(\tilde{\theta}_2)] = p(\tilde{\theta}; \sigma_\theta) \delta(\tilde{\theta}_1 - \tilde{\theta}_2)$ ,  $p(\tilde{\theta}; \sigma_\theta)$  can be understood as the spatial power distribution of the distribution source.

In fact, the distributed model established by (45) can be explained by the model (43) mentioned in the previous section, and taking  $b(k) = \int_{-\pi}^{\pi} f(\theta, k) a(\theta) d\theta$  in it, we can obtain:

$$z(k) = s(k) \int_{-\pi}^{\pi} f(\theta, k) a(\theta) d\theta + n(k), k \in Z \quad (46)$$

Compared with two formulas, it is not difficult to see that both of described model is consistent. The ship target echo signal vector  $s(t) = [s_1(t), s_2(t), \dots, s_q(t)]^T$  and noise vector  $n(t)$  are independent random vectors of zero-mean, and through the multi-dimensional spectrum peak search, their second moment are respectively:

$$E[s_r s_k^H] = P_s \delta(t, k), E[n_r n_k^H] = \sigma_n^2 I_M \delta(t, k) \quad (47)$$

Among them,  $\delta(t, k)$  is the kronnecker  $\delta$  function.  $P$  is the signal covariance matrix, and  $I_M$  is the M-order unit matrix.  $\sigma_n^2$  is the noise variance.

The covariance matrix of the observed data vector  $z(t)$  can be represented as:

$$R = E[z(t) z^H(t)] = B P_s B^H + \sigma_n^2 I_M \quad (48)$$

Among them,  $B = [b_1(\theta_1), b_2(\theta_2), \dots, b_q(\theta_q)]^T$ , the singular value of covariance matrix is decomposed into:

$$R = U_s \Lambda_s U_s^H + U_n \Lambda_n U_n^H \quad (49)$$

The column vectors of matrix  $U_s$  and  $U_n$  are respectively composed of singular values  $\sigma_1, \sigma_2, \dots, \sigma_q$  and corresponding singular vectors of  $\sigma_n$ . Moreover  $\sigma_1 \geq \sigma_2 \geq \dots \geq \sigma_q > \sigma_n$ , supposing that there is no correlation between the different distribution sources, namely  $U_n^H b_i(\theta_i) = 0$ , the orthogonality of the direction vector and the noise subspace. By using this method, we can obtain a multidimensional spectral peak search method of DOA estimation method of ship far small infrared targets:

$$f(\phi) = \frac{1}{b^H(\phi) \hat{U}_n U_n^H b(\phi)} \quad (50)$$

Supposing that the angular signal distribution function of the distributed target source is known, and the specific expression is determined by unknown parameter  $\phi_i$ .  $\phi_i$  is the vector of multiple parameters. According to the formula (50), the distributed target DOA and other unknown parameters can be obtained by multi-dimensional parameter spectral peak search.

### JOINT PARAMETER ESTIMATION ALGORITHM OF SHIP TARGET LOCATION

The multidimensional spectrum peak search algorithm is the extension of the MUSIC algorithm in the estimation of distributed target [30]. The theoretical basis is basically the same. According to the principle, we carry out the central direction of arrival and extended angle estimation of far small infrared targets of ship. If the unknown parameters of signal source only has two, namely the central direction of arrival  $\theta_i$  and expansion  $\sigma_i$ , the above method becomes the solution of the minimization problem:

$$(\theta_i, \sigma_i) = \arg \min b_i^H(\theta, \sigma) \hat{U}_n U_n^H b_i(\theta, \sigma) \quad (51)$$

For several common forms of distribution, they all satisfy:

$$b_i(\theta_i) = \Phi(\theta_i) h_i \quad (52)$$

Among them, the  $M$ -order diagonal matrix  $\Phi(\theta_i) = \text{diag}(a(\theta_i))$  and  $M$ -order vector  $h_i = \int_{-\pi}^{\pi} a(\theta) g_i(\theta) d\theta$  can prove that if the signal source angle signal distribution function  $g_i(\theta)$  is conjugate symmetric function, that is  $g_i(\theta) = g_i^*(-\theta)$ , the vector  $h_i$  is the real vector, that is  $h_i \in \mathbb{R}^M$ , the vector is the real vector. Combined (52) formulas with (3-8) formulas, the distributed target DOA becomes the solution of the minimization problem as follows:

$$(\theta_i, \sigma_i) = \arg \min h_i^H \Phi^H(\theta) \hat{U}_n U_n^H \Phi(\theta) h_i \quad (53)$$

Let  $Q_1(\theta) = \Phi^H(\theta) \hat{U}_n U_n^H \Phi(\theta)$ , we can see that the minimum eigenvalue of the matrix  $Q_1(\theta)$  takes the minimal value for the distributed target DOA.  $h(\sigma_i)$  is the corresponding eigenvector, and it is the real vector. The matrix  $Q_1(\theta)$  is non negative conjugate symmetric matrix, and the eigenvalues are non negative, so the distributed target DOA estimation corresponds to the spectral peak position of the following spatial spectrum.

$$f_1(\theta) = -\log_{10}(\lambda_{\min}[Q_1(\theta)]) \quad (54)$$

By searching the minimum eigenvalue, one-dimensional DOA estimation of the coherent distributed target is obtained. For the common form of distribution source position distribution,  $b_i(\theta_i) = G_i a(\theta_i)$ , among them,  $G_i$  is the  $M$ -order diagonal matrix and  $G_i = \text{diag}([h_{i1}, h_{i2}, \dots, h_{iM}])$  is only related to the distribution degree of the ship target, which

is not related to DOA of the target. When the distribution of  $\theta_{ik}$  is about the symmetrical distribution of  $\theta_i$ , all of  $h_{i1}, h_{i2}, \dots, h_{iM}$  are real numbers. The covariance matrix and singular value decomposition of the observed data vector can deduce  $BPB^H = U_s(\Lambda_s - \Lambda_s)U_s^H$ , and thus  $B$  can be transformed into  $B = U_s W$ , among them, is the  $q \times q$ -order nonsingular matrix.

From the above analysis, we can get the following equation:

$$\begin{bmatrix} h_{i1}^* h_{i2} e^{-j2\pi(d/\lambda)\sin\theta_i} \\ h_{i2}^* e^{j\theta_i} h_{i3} e^{-j2\pi(d/\lambda)\sin\theta_i} \\ \dots \\ h_{i(M-1)}^* e^{j(M-2)\times 2\pi(d/\lambda)\sin\theta_i} h_{iM} e^{-j(M-1)2\pi(d/\lambda)\sin\theta_i} \end{bmatrix} = \begin{bmatrix} (u_1^H w)^* u_2^H w \\ (u_2^H w)^* u_3^H w \\ \dots \\ (u_{M-1}^H w)^* u_M^H w \end{bmatrix} \quad (55)$$

$u_1, u_2, \dots, u_M$  is the row vector of  $U_s$ ,  $w$  is  $i$ -th column vector of  $W$ . Because  $h_{i1}, h_{i2}, \dots, h_{iM}$  are real numbers, from the above formula we can get:

$$\begin{bmatrix} (u_1^H w)^* u_2^H w \\ (u_2^H w)^* u_3^H w \\ \dots \\ (u_{M-1}^H w)^* u_M^H w \end{bmatrix} = e^{-j2\pi(d/\lambda)\sin\theta_i} \begin{bmatrix} (u_2^H w)^* u_1^H w \\ (u_3^H w)^* u_2^H w \\ \dots \\ (u_M^H w)^* u_{M-1}^H w \end{bmatrix} \quad (56)$$

Which can also be expressed as:

$$u_k^H w w^H u_{k-1} = e^{-j2\pi(d/\lambda)\sin\theta_i} u_{k-1}^H w w^H u_k \quad (57)$$

From above formulas, it only keeps the information which is related to distributed object DOA, and does not keep the information which is related to degree of distribution. Thus positioning estimation algorithm of the ship far small infrared targets based on the distributed target position estimation and DOA location:

1) estimate the covariance matrix of observed data  $\hat{R} = \frac{1}{N} \sum_{i=1}^N x_i x_i^H$ ,  $N$  is independent number of snapshots, perform the singular value decomposition on  $R$ , obtain the number of signal subspace  $U_s$  and number of distributed target  $q$ .

$$2) \text{ Let: } P_1 = \begin{bmatrix} u_1^T \otimes u_2^H \\ u_2^T \otimes u_1^H \\ \dots \\ u_{M-1}^T \otimes u_M^H \end{bmatrix}, P_2 = \begin{bmatrix} u_2^T \otimes u_1^H \\ u_3^T \otimes u_2^H \\ \dots \\ u_M^T \otimes u_{M-1}^H \end{bmatrix}, v = \text{vec}(w w^H) \quad (58)$$

The row vectors of  $U_s$  are plugged into (57), and  $P_2$  are computed, and then the generalized eigenvalue decomposition is computed:

$$P_1^H P_1 [v_1, v_2, \dots, v_{q \times q}] = \text{diag}(\alpha_1, \alpha_2, \dots, \alpha_{q \times q}) P_1^H P_2 [v_1, v_2, \dots, v_{q \times q}] \quad (59)$$

We use  $q$  phase angles of eigenvalues of model which is close to 1 to estimate DOA of distributed ship targets, so as to realize the joint estimation of the distance of ship target, DOA and frequency parameters, then realizing the classification recognition of ship target through computer recognition and machine learning classification algorithm.

## SIMULATION EXPERIMENT AND RESULT ANALYSIS

In order to test application performance of the proposed algorithm in realizing the positioning and recognition of ship far small infrared targets, we need a simulation experiment. The experiment uses Matlab 7 simulation design, supposing that the point distribution model of ship far small infrared targets is composed of the uniform line array which is composed of 14 array elements. The array element spacing is 0.25 times of minimum wavelength [31,32]. The signal source is two complex exponential signals with equal power. The signal frequencies are respectively 200Hz, 100Hz. The sampling frequency is 2000Hz. The signal-to-noise ratio is 10dB. Two far small infrared target signals of ship are  $10^\circ$  and  $30^\circ$ . The number of snapshots is 200. The replication number of experiment is 50 times. The distributed target signal source reach to the array respectively from the  $\theta_1 = 4^\circ, \theta_2 = 7^\circ$  direction of arrival. Expansion of two signal source respectively is  $\Delta_1 = 1^\circ, \Delta_2 = 2^\circ$ , and the signal to noise ratio of surge interference is 10. The number of snapshots

of surge is 1000. The noises are white Gaussian noise and Gaussian colored noise [33]. Gaussian colored noise is formed

through a two order AR model of  $H(z) = \frac{z^{-2}}{1 - a_1 z^{-1} + a_2 z^{-2}}$ , among them,  $a_1 = 2\rho \cos(2\pi f_n / f_s), a_2 = \rho^2, 0 < \rho < 1, \rho$

is a coefficient responding spectrum width. According to the simulation environment and parameter settings, the searching results of the power spectrum of the ship's far small infrared target position estimation is obtained in surge interference are shown in Fig. 3. In this paper, the location search results after suppression of surge interference using the proposed method are shown in Fig. 4.

Compared with Figures 3-4, we can see that using this method for ship far small infrared target recognition, two spectrum peaks are respectively corresponding to 10 degrees and 30 degrees in horizontal ordinate, but they are different between them. The accuracy of target location is not good without surge interference suppression processing. From the average results of 50 experiments.

We can see that through the surge interference suppression, the spectral peak of target location estimation is much sharper, and the position estimation of ship target is more accurate which is easy to distinguish the signal which has a small difference in the two azimuth angles, so as to effectively achieve the accurate identification of ship far small infrared.

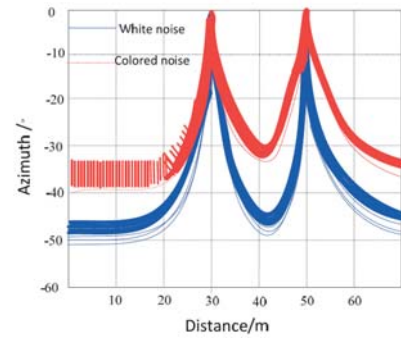


Fig. 3. Estimation result of locating and searching power spectrum intensity of ship target under surge interference.

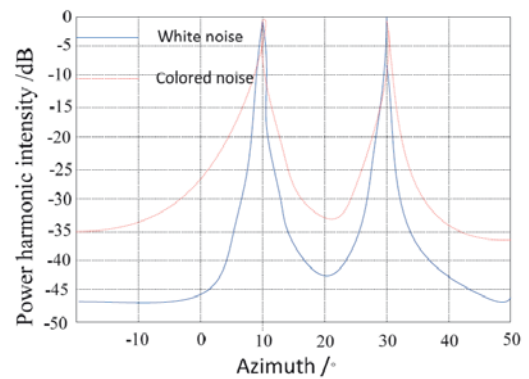


Fig. 4. Location search results after suppression of surge interference with using the proposed method.

In order to compare the performance of different methods, we further test the estimation results of azimuthal angle for ship far infrared target localization in this method and the traditional methods, and comparison results are shown in Fig. 5.

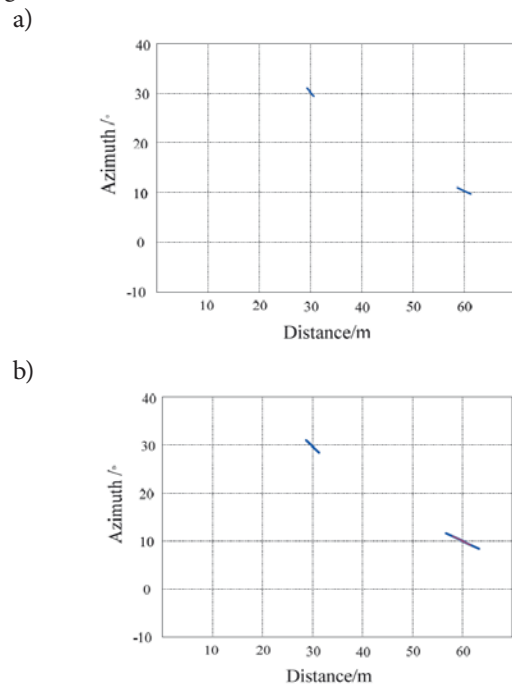


Fig. 5. Contrast results of azimuthal angle of ship far small infrared target localization. (a) Traditional two-dimensional MUSIC method (b) Proposed method in this paper



Simulation results show that the corresponding abscissas of the two spectrum peaks are 30 m and 60 m, and the corresponding ordinates are 30 degrees and 10 degrees in Fig. (a). The azimuth angle and distance of the two sources can be seen more directly from (b). But there is the difference between them. Compared with (a), we can see that the spectral peak of Gauss white noise is more sharp than the color noise environment. From (b) we can see that compared with the white noise with the color noise environment, the DOA estimation result of ship targets are more accurate, and the estimation error is low. Therefore, using the computer recognition method for target recognition of ship, the root-mean-square error  $\bar{E}$  comparison of the three kinds of ship far small infrared target recognition is shown in Table 1. The analysis of Table 1 shows that the error of proposed method for ship target recognition is low, and has better accuracy.

### CONCLUSIONS

The location recognition method of far small infrared target recognition algorithm of ship was studied in this paper. This paper proposed far small infrared target recognition algorithm of ship based on distributed target position estimation and DOA location in computer vision model for constructing coherent distributed source array model of far small infrared target distribution of ship. This algorithm used MUSIC algorithm for the beamforming processing of far small infrared target echo model of ship. Combined with the adaptive filtering algorithm we carried out the surge interference suppression and the estimation of central direction of arrival and angle spread of far small infrared target of ship through multidimensional spectrum peak searching algorithm, realizing the joint estimation of distance of ship target, DOA and frequency parameters, so as to realize the accurate positioning and recognition of targets. Simulation results show that using this method for the far small infrared target recognition of ship under surge interference, the spectral peak sharpness of spectral peak search of target position is high, side-lobe suppression performance is good, which shows the high accuracy of target position estimation and location, the accuracy and anti-interference performance of far small infrared target recognition of ship is good. Through the computer recognition method, we achieves smaller errors of far small infrared target recognition of ship, improving the accurate recognition ability

of ship target, and it has good application value of realizing the precision strike of ship target.

### REFERENCE

1. K. Zhong, H. Peng, L. D. Ge, 2015. Blind Equalization Based on FABA-SISO for Continuous Phase Modulation Signals over Time-varying Frequency-selective Fading Channels. JEIT, 37(11): 2672-2677.
2. Z. F. Shu, X. K. Dou, H. Y. Xia, et al. 2012. Low stratospheric wind measurement using mobile rayleigh doppler wind LIDAR. Journal of the Optical Society of Korea, 16(2): 141-144
3. R. Wang, Y. Ma, 2014. DOA Estimation of Wideband Linear Frequency Modulated Pulse Signals Based on Fractional Fourier Transform. Acta Armamentarii, 35(3): 421-427.
4. Y. Bengio, A. Courville, P. Vincent, 2013. Representation learning: a review and new perspectives. IEEE Transactions on Pattern Analysis and Machine Intelligence, 35(8): 1798-1828.
5. Z. Chen, J. Chen, 2014. The Design of Optimized Android Salvation Platform Based on Multi-State Visual Identity. Bulletin of Science and Technology, (4): 62-64.
6. J. L. Pan, Z. Xiong, L. N. Wang, 2015. Etal A Simplified UKF Algorithm for SINS/GPS/CNS Integrated Navigation System in Launch Inertial Coordinate System. Acta Armamentarii, 36(3): 484-491.
7. H. Y. Shi, N. Zhang, 2015. Moving Targets Indication Method in Single SAR Imagery Based on Sparse Representation and Road Information. Chinese Journal of Electronics, 43(3): 431-439.
8. Y. Y. Yao, L. Tang, 2016. Robot Visual Path Following Identification Optimization Simulation. Computer Simulation, 33(5):401-404.

Tab. 1. Comparison results of root mean square error of far and small infrared target recognition of ship.

Target	1	2	3	4	5	6	7	8	$\sigma$	$\bar{E}$
Proposed method	0.368	0.375	0.305	0.428	0.320	0.532	0.415	0.494	0.083	0.399
Two-dimensional MUSIC method	1.179	1.702	1.921	1.350	2.037	1.931	1.400	1.046	0.402	1.466
High order spectrum feature extraction method	0.870	0.755	0.799	0.861	0.884	0.614	0.635	0.639	0.133	0.716

9. Y. Ding, H. Dai, S. Wang, 2014. Image quality assessment scheme with topographic independent components analysis for sparse feature extraction. *Electronics Letters*, 50(7): 509-510.
10. L. C. Manikandan, R. K. Selvakumar, 2014. A new survey on block matching algorithms in video coding. *International Journal of Engineering Research*, 3(2): 121-125.
11. H. Bdi, L. J. Williams, 2010. Principal component analysis. *Wiley Interdisciplinary Reviews: Computational Statistics*, 2(4): 433-459.
12. J. Z. Jiang, X. L. Cheng, S. Ouyang, 2015. Fast Design of Double-prototype Discrete Fourier Transform Modulated Filter Banks. *JEIT*, 37(11): 2628-2633.
13. F. Ma, 2016. A license plate location algorithm based on wavelet transform and Tophat transform. *Electronic Design Engineering*, 24(22): 118-121.
14. N. Rajapaksha, A. Madanayake, L. T. Bruton, 2014. 2D space- time wave-digital multi-fan filter banks for signals consisting of multiple plane waves. *Multidimensional Systems and Signal Processing*, 25(1): 17-39.
15. X. Y. Jin, X. Y. Zhou, Zhang W. L. 2014. Modulation Recognition Using Adaptive MCMC in Multipath Fading Channel, Modulation Recognition Using Adaptive MCMC in Multipath Fading Channel. *Journal of Beijing University of Posts and Telecommunications*, 37(1): 31-34.
16. S. L. Xie, Y. Liu, J. M. Yang, et al. 2012. Time-Frequency Approach to Underdetermined Blind Source Separation. *IEEE Transactions on Neural Networks and Learning Systems*, 23(2): 306-315.
17. V. M. Alfaro, R. Vilanovab, 2013. Robust tuning of 2DoF five-parameter PID controllers for inverse response controlled processes. *Journal of Process Control*, 23(4): 453-462.
18. C. Y. Tuo, 2015. An Improved Localization Algorithm for Radio Frequency Identification Reader. *Computer Measurement & Control*, 23(3).
19. P. frihauf, M. Krstic, T. Basar, 2012. Nash equilibrium seeking in Noncooperative games. *IEEE Transaction on Automatic Control*, 57(5): 1192-1207.
20. M. R. Hesamzadeh, D. R. Biggar, 2012. Computation of extremal-Nash equilibria in a single-stage MILP. *IEEE Transaction on Power System*, 27(3): 1706-1707.
21. K. Oberleithner, M. Sieber, C. N. Nayeri, et al. 2011. Three-dimensional coherent structures in a swirling jet undergoing vortex breakdown: stability analysis and empirical mode construction. *Journal of Fluid Mechanics*, 679(1): 383-414.
22. T. Li, P. Gopalakrishnan, R. Garg, M. Shahnam, 2012. CFD-DEM study of effect of bed thickness for bubbling fluidized beds. *Particuology*, 10(5): 532-541
23. X. H. Lu, R. J. Chen, K. D. Chi, 2016. A Rescue Robot Perception System with Introduction of Infrared Heat Release Detection in Human Body. *Ship Electronic Engineering*, 36(3): 151-155.
24. K. Liu, J. H. Zhu, B. Yu, 2013. Longitudinal control of aircraft with thrust vectoring using robust dynamic inversion. *Control and Decision*, 28(7): 1113-1116.
25. Gao, W. and W. Wang, The fifth geometric-arithmetic index of bridge graph and carbon nanocones. *Journal of Difference Equations and Applications*, 2017. 23(1-2SI): p. 100-109.
26. Gao, W., et al., Distance learning techniques for ontology similarity measuring and ontology mapping. *Cluster Computing-The Journal of Networks Software Tools and Applications*, 2017. 20(2SI): p. 959-968.
27. Z. Zheng, L. Y. Wang, Y. Zhou, 2013. Chaos Theory and Its Application in Ships Target Recognition. *Ship Electronic Engineering*, 33(5): 48-50.
28. M.A. Hassan, M.A.M. Ismail, 2017. Literature Review for The Development of Dikes's Breach Channel Mechanism Caused by Erosion Processes During Overtopping Failure. *Engineering Heritage Journal*, 1(2): 23-30.
29. H. Yasin, M. Usman, H. Rashid, A. Nasir, A. Sarwar, I.A. Randhawa, 2017. Guidelines for Environmental Impact Assessment of JHAL flyover and underpass project in Faisalabad. *Geology, Ecology, and Landscapes*, 1(3): 205-212.
30. R. Radmanfar, M. Rezayi, S. Salajegheh, V.A. Bafrani, 2017. Determination the most important of hse climate assessment indicators case study: hse climate assessment of combined cycle power plant staffs. *Journal CleanWAS*, 1(2): 23-26.
31. I. Ismail, M.L. Husain, R. Zakaria, 2017. Attenuation of Waves from Boat Wakes in Mixed Mangrove Forest of Rhizophora And Bruguiera Species In Matang, Perak. *Malaysian Journal Geosciences*, 1(2):32-35.
32. H.F. Soehady, J. Asis, S. Tahir, B. Musta, M. Abdullah, H. Pungut, 2017. Geosite Heritage and Formation Evolution of Maga Waterfall, Long Pasia, South of Sipitang, Sabah. *Geological Behavior*, 1(2):34-38.

33. S.B. Shamsudin, A. Marzuki, M.S. Jeffree, K.A. Lukman, 2017. Blood lead concentration and working memory ability on malay primary school children in urban and rural area, Malacca. Acta Scientifica Malaysia, 1(1): 04-07.

#### **CONTACT WITH THE AUTHOR**

Renping Zhu

*e-mail: xgczrp@ncu.edu.cn*

Department of Admission and Employment Office  
Nanchang University  
Nanchang 330031  
**CHINA**